9-11-2020

Mechanism and Chemoselectivity for HOCl-Mediated Oxidation of Zinc-Bound Thiolates

Lindsay Zumwalt

Arden Perkins

O. Maduka Ogba

Mechanism and Chemoselectivity for HOCl-Mediated Oxidation of Zinc-Bound Thiolates

COMMUNICATION

Mechanism and Chemoselectivity for HOCl-Mediated Oxidation of Zinc-Bound Thiolates

Lindsay Zumwalt,[a] Arden Perkins,[b] and O. Maduka Ogba*[a]

[a] L. Zumwalt, Prof. Dr. O. M. Ogba
Chemistry and Biochemistry Program, Schmid College of Science and Technology
Chapman University
One University Drive, Orange, CA 92866
E-mail: ogba@chapman.edu

[b] Dr. A. Perkins
Institute of Molecular Biology
University of Oregon
1585 E 13th Ave, Eugene, OR 97403

Supporting information for this article is given via a link at the end of the document.

Abstract: Quantum mechanical calculations reveal the preferred mechanism and origins of chemoselectivity for HOCl-mediated oxidation of zinc-bound thiolates implicated in bacterial redox sensing. Distortion/interaction models show that minimizing geometric distortion at the zinc complex during the rate-limiting nucleophilic substitution step controls the mechanistic preference for OH over Cl transfer with HOCl and the chemoselectivity for HOCl over H_2O_2.

Zinc-thiolate complexes play a central role in bacterial defense mechanisms against hypochlorous acid (HOCl) – one of the most potent oxidants produced by animal host systems through the neutrophilic oxidative burst.[1–3] Proteins that contain the $[Zn(Cys)_x(His)_y]$ architecture (where x + y = 4) are implicated in HOCl sensing through a reversible oxidation process at the zinc-bound cysteine(s), launching redox signaling cascades that can regulate protein activity,[4] mitigate protein aggregation,[5] increase bacterial resistance,[6] and alter bacterial localization.[7] While the reactivity of zinc-bound thiolates to oxidants such as H_2O_2 is well documented via experimental[8,9] and theoretical studies,[10,11] comparable work with HOCl is still in its infancy.[12] Furthermore, apart from modulating the protonation state[13] and nucleophilicity[14] of the bound thiolate at physiological pH, no additional role of Zn^{2+} complexes in governing the reactivity of the bound thiolates toward oxidants has been explored.

We recently reported the HOCl-sensing function of a chemoreceptor zinc-binding (CZB) domain[15] – $[Zn(Cys)(His)_3]$ – in the chemoreceptor transducer-like protein D (TlpD) of *Helicobacter pylori* implicated in the chemoattractant response of the gastric pathogen to micromolar concentrations of HOCl (Figure 1A).[7] We showed that this 3His/1Cys system selectively senses HOCl through oxidation of the single zinc-bound cysteine to sulfenic acid. This results in localized unraveling in the helix containing the zinc-binding cysteine to reversibly inactivate the chemoreceptor and promote a bacterial swimming response to facilitate chemoattraction. These CZB domains present a unique opportunity to study zinc-thiolate reactivity with HOCl, as high-resolution experimental structures offer a pristine view of the zinc-binding core, and they contain a single reactive cysteine, as opposed to other systems, such as zinc-finger proteins,[12] that contain multiple cysteines and undergo complicated disulfide shuffling. Furthermore, CZB domains are present in numerous bacteria, including many enteric pathogens, and so understanding their molecular function has relevance for human diseases.[15] However, it remains unknown how the Zn^{2+} complex mediates the redox mechanism and the exquisite HOCl-sensing over other biological oxidants.

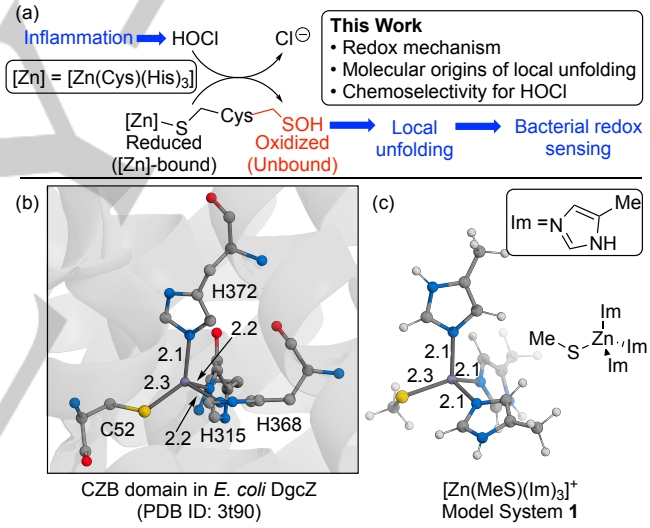

Figure 1. (a) Experimental model for the CZB HOCl-sensing response and study aims. (b) Crystal structure of the CZB domain in *E. coli* DgcZ solved at 2.20 Å resolution. (c) Model $[Zn(MeS)(Im)_3]^+$ system **1** used in this study.

Herein, we report the first computational study of the mechanism for HOCl-mediated oxidation of zinc-bound thiolates. We provide new insights into the role of the Zn^{2+} complex in mediating the reaction pathway and the chemoselectivity for HOCl over H_2O_2. We discuss the role of the chloride by-product in facilitating the observed local unfolding of the CZB domain upon oxidation.

All computational results reported herein were conducted using *Gaussian 16*.[16] Quantum mechanical (QM) geometry optimizations and vibrational frequency calculations were performed in vacuum using B3LYP[17]/SDD[18](Zn)/6-31+G(d,p)[19–21] level of theory. Single point energies were calculated using M06[22] with the identical mixed basis sets used for optimizations.[23] Stationary points were verified through

vibrational frequency analysis. Intrinsic reaction coordinate (IRC) analysis[24,25] of each transition state confirmed connecting minima along the reaction coordinates.[26] All energies were calculated at 298 K and 1.0 atm.

HOCl-sensing is conserved across representative CZB domains,[7] indicating that the mechanism is localized at the conserved 3His/1Cys Zn^{2+} core. Therefore, we designed a model system for computational analyses from the crystal structure of the core CZB domain in *E coli* diguanylate cyclase Z solved at 2.20 Å resolution (DgcZ, PDB ID: 3t9o, Figure 1B).[27] The C_α–C_β bond of each zinc-ligated residue was cut, and the C_β replaced with methyl groups, resulting in a cationic $[Zn(MeS)(Im)_3]^+$ complex **1** optimized to a structure with Zn-S and Zn-N bond lengths consistent with the crystal structure (Figure 1C).

Next, we computed the reaction pathway for HOCl-mediated oxidation of **1** (Figure 2A). Coordination of HOCl to **1** forms **2** (ΔG = 1.0 kcal/mol) held by an O-H•••S interaction. Reorganization of HOCl and subsequent nucleophilic substitution is rate-limiting (**TS-3**, OH transfer, $\Delta G^‡$ = 8.3 kcal/mol). From IRC analysis, **TS-3** leads to a zinc-bound methane sulfenic acid **4** (ΔG = –29.7 kcal/mol) ligated to the Zn^{2+} at the oxygen and coordinated to the chloride ion by-product via hydrogen bonding.[28] The computed barrier is consistent with the experimentally observed rate-constant approaching the diffusion limit for a related system.[12] Exchange of methane sulfenic acid with chloride to form **6** was facile (**TS-5**, $\Delta G^‡$ = 1.3 kcal/mol) and exergonic by 13.8 kcal/mol,[29] indicating that the chloride-induced release of the oxidized thiolate is favored, and may initiate the local unfolding at the CZB domain.

Previous studies on HOCl-mediated oxidation of "free" cysteines invoke a Cl transfer mechanism that proceeds through a sulfenyl chloride intermediate,[1,30–33] although a report has called this intermediate into question.[34] We investigated this pathway in our zinc-bound system (Figure 2A). Upon HOCl coordination, a rearranged complex **7** (ΔG = 3.4 kcal/mol) was located. Nucleophilic substitution (Cl transfer) from **7** proceeds through the rate-limiting **TS-8** ($\Delta G^‡$ = 14.4 kcal/mol). IRC analysis from **TS-8** reveals that nucleophilic substitution occurs concurrently with initial *S*- to *Cl*- linkage isomerization at the Zn^{2+}, followed subsequently by exchange of the newly formed sulfenyl chloride with the hydroxide at the Zn^{2+} to form **9**.[26] Rearrangement of **9** leads to **10** preorganized for subsequent sulfenic acid formation. Complex **10** undergoes nucleophilic substitution of the chloride by the zinc-bound hydroxide (**TS-11,** $\Delta G^‡$ = 6.8 kcal/mol) to form **4**. The data show that for zinc-bound thiolates, OH transfer is more kinetically favored over Cl transfer by 6.1 kcal/mol, equivalent to a relative rate of ~30000:1 favoring OH transfer at 298 K as estimated via the Eyring equation.

In the OH (**TS-3**) and Cl transfer (**TS-8**) transition states, the thiolate S, transferring group, and leaving group are linear – a typical S_N2 process (Figure 2B). The leaving group is stabilized via ionic C-H•••X interactions[35–37] (X = Cl for **TS-3**; X = OH for **TS-8**) with the imidazole ligands. Structural deviations are apparent upon closer observation. In **TS-3**, the Zn-S distance is 2.3 Å, virtually undistorted from **1** while in **TS-8**, significant Zn–S elongation of 0.7 Å is observed. Furthermore, the proximity of the OH transferring group to Zn in **TS-3** is 3.0 Å while the corresponding Cl•••Zn distance in **TS-8** is 2.5 Å. The oxidant O-Cl bond is also further elongated in **TS-8** than in **TS-3**. Globally, the Zn^{2+} complex in **TS-3** retains a tetrahedral geometry from complex **1**, while a trigonal bipyramid geometry is observed in **TS-8**. Taken together, the zinc complex appears to be preorganized for OH transfer but require significant reorganization for Cl transfer.

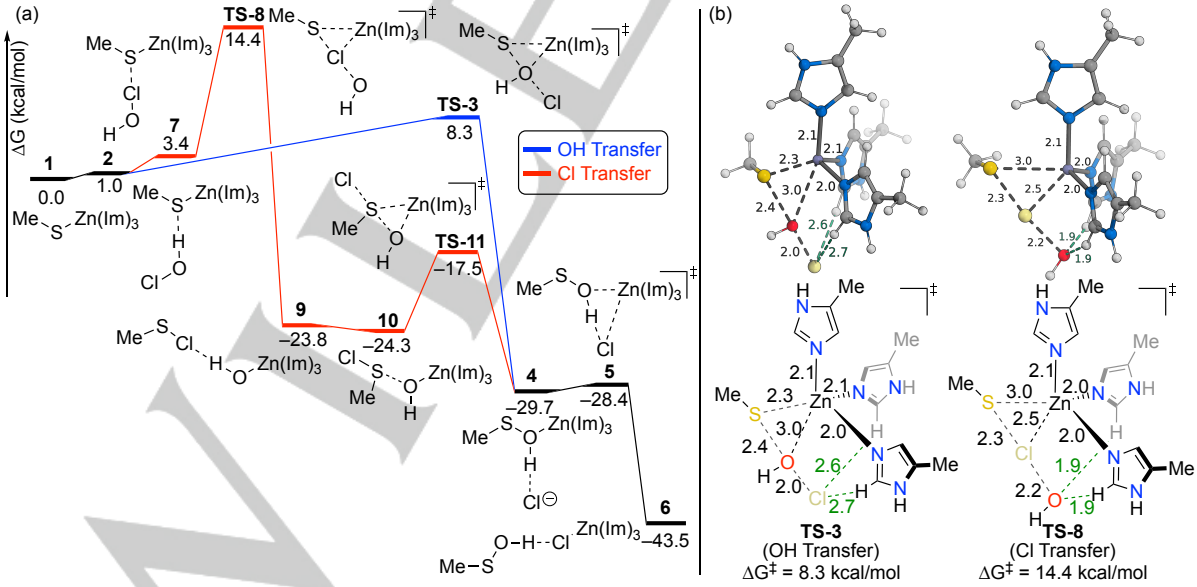

Figure 2. (a) QM computed HOCl-mediated oxidation of **1**. Two transfer mechanisms, OH transfer and Cl transfer, are reported. The former is kinetically favored over the latter by 6.1 kcal/mol. (b) The rate-limiting transition state geometries for both OH (**TS-3**) and Cl (**TS-8**) transfer. Distances are reported in Ångströms (Å).

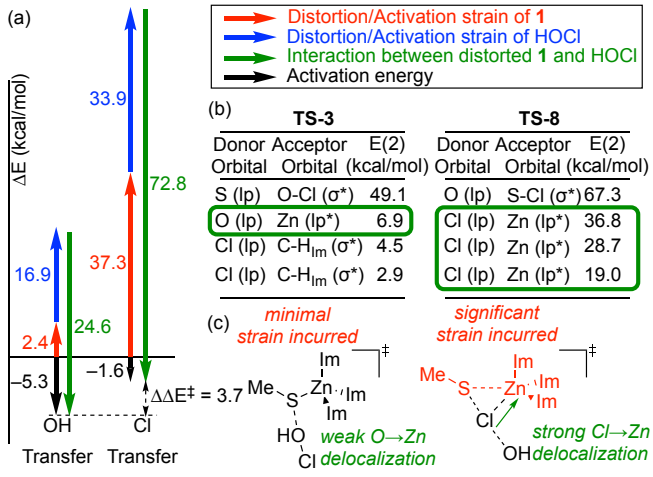

Figure 3. (a) Distortion/interaction models for OH (**TS-3**) and Cl (**TS-8**) transfer. (b) NBO 2nd order perturbation energies – E(2) – in **TS-3** and **TS-8** (top four most significant presented). (c) Reactivity model for the mechanistic preference for OH over Cl transfer.

Distortion/interaction (D/I) models[38] were calculated to elucidate the origins of this mechanistic preference (Figure 3A). The activation electronic energy ($\Delta E^{\ddagger}$) to reach **TS-3** (OH transfer) and **TS-8** (Cl transfer) was decomposed into the activation strain (or distortion energy) and the interaction energy between distorted reactants.[26] Activation strain for OH transfer is significantly less by 51.9 kcal/mol than that for Cl transfer, consistent with the transition state geometries. In both, interaction between distorted reactants override the distortion energies. However, the relative magnitude of interaction with respect to distortion for OH transfer is 3.7 kcal/mol greater than that for Cl transfer. This energetic difference alone accounts for 61% of the observed selectivity.

Natural bond orbital (NBO)[39] 2nd order perturbation (i.e., hyperconjugation) energies reveal the origins of the interaction energy differences between both OH and Cl transfer mechanisms (Figure 3B). In this analysis, we focus on the most significant donor-acceptor orbital interaction energies between the oxidant and the zinc complex. For both mechanisms, the largest interaction occurs at atoms involved in the bond forming/breaking S_N2 process. However, for Cl transfer (**TS-8**), several significant Cl to Zn^{2+} orbital delocalization interactions are observed while the analogous O to Zn^{2+} orbital delocalization in OH transfer (**TS-3**) is relatively weak. This indicates that the large interaction energy observed via D/I models during Cl transfer is due to strong orbital delocalization from the transferring Cl to the Zn^{2+} center.

D/I and NBO analyses reveal a reactivity model for HOCl-mediated oxidation of zinc-bound thiolates (Figure 3C). The Zn^{2+} complex and oxidant during Cl transfer are more severely distorted but interact more intimately than during OH transfer. However, the strain incurred from the distortion more significantly outweighs the stabilizing Cl to Zn^{2+} interactions during Cl transfer. This leads us to conclude that the preference for OH over Cl transfer within the context of zinc-bound thiolates is more strongly governed by minimizing geometric strain than by maximizing interactions.

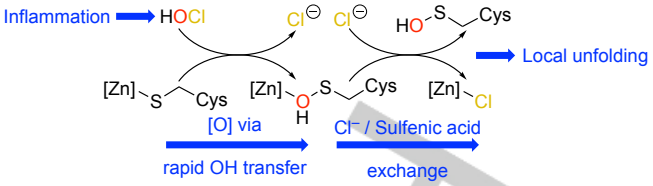

Figure 4. Updated model for CZB HOCl-sensing in bacteria.

We propose a revised model for the observed unraveling at CZB domains in the presence of HOCl (Figure 4). HOCl-mediated oxidation occurs via rapid OH transfer and forms zinc-bound sulfenic acid and chloride ion as by-product. Release of sulfenic acid from the Zn^{2+} complex is facilitated by exchange with the chloride, which disrupts the key zinc-cysteine Lewis acid-base interactions and promotes local unfolding within the CZB domain.

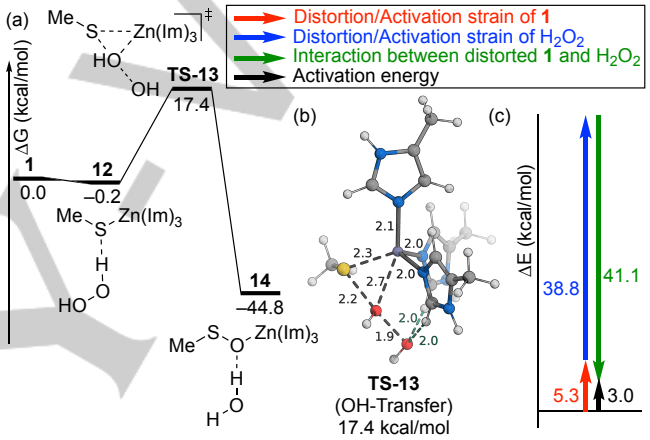

Figure 5. (a) H_2O_2-mediated oxidation of **1**. (b) The rate-limiting transition state geometry. Distances are reported in Ångströms (Å). (c) Distortion/Interaction analysis for **TS-13**.

Next, we compared the HOCl-mediated process with that of H_2O_2 to understand the experimentally observed chemoselectivity (Figure 5A). H_2O_2-mediated oxidation begins with the coordination of the oxidant with **1** (ΔG = –0.2 kcal/mol) to form **12**. The rate-limiting nucleophilic substitution (**TS-13**, $\Delta G^{\ddagger}$ = 17.6 kcal/mol) occurs concurrently with proton transfer to form **14** (ΔG = –44.8 kcal/mol). The concurrent nucleophilic substitution and proton transfer is verified via IRC analysis from **TS-13**[26] and is consistent with previous computational reports.[10,11,40] Altogether, the HOCl-mediated process is favored over H_2O_2 by 9.3 kcal/mol, consistent with all previous experimental observations.[7,12,4]

The rate-limiting step for H_2O_2-mediated oxidation is inherently an OH transfer, akin to that observed in the preferred pathway with HOCl. Accordingly, the transition state geometry in the former (**TS-13**, Figure 5B) resembles that of the latter (**TS-3**, Figure 2B), and the similarity is confirmed via D/I models revealing a similarly distorted complex **1** in both (Figure 5C vs. 3A). However, D/I models show that H_2O_2 is more significantly distorted than HOCl during OH transfer to reach **TS-13**. To confirm that selectivity is localized at the oxidant, we compared the free energy barriers for this elementary OH transfer step to the analogous process with an unbound "free" methanethiolate (Figure 6). In the zinc-bound system, the barrier difference is 10.3

kcal/mol favoring HOCl over H_2O_2. With "free" methanethiolate, a 14.0 kcal/mol barrier difference favoring HOCl is observed. The data show that upon controlling for OH transfer by the Zn^{2+} complex, selectivity for HOCl- over H_2O_2 is based mostly on differences in leaving group tendencies of the chloride vs. the hydroxide in the S_N2 process.

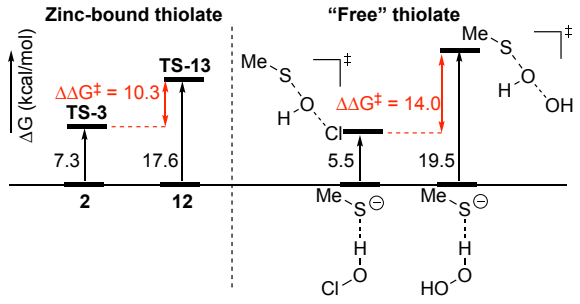

Figure 6. QM computed barriers for the elementary OH transfer step of HOCl- and H_2O_2- mediated oxidation of **1** and "free" methanethiolate. The complexed reactants are the zero of energy reference across the four systems.

The detailed mechanism and origins of chemoselectivity for HOCl-mediated oxidation of zinc-bound thiolates has been presented. Both reactivity and selectivity are predicated on minimizing geometric distortion during the rate-limiting nucleophilic substitution step. A ligand exchange model is proposed for the observed local unfolding of these HOCl-sensing CZB domains upon oxidation; a redox-sensing mechanism that may be used by many bacteria that colonize humans and other animals to respond to host inflammation.

Acknowledgments: We acknowledge Chapman University's Information Systems and Technology Research Technology Support team for provision and maintenance of the high-performance computing facility utilized for this work.

Keywords: Density functional calculations • Redox chemistry • Reaction mechanisms

[1] M. J. Gray, W.-Y. Wholey, U. Jakob, *Annu. Rev. Microbiol.* **2013**, *67*, 141–160.
[2] C. C. Winterbourn, A. J. Kettle, *Antioxid. Redox Signal.* **2012**, *18*, 642–660.
[3] S. J. Weiss, *N. Engl. J. Med.* **1989**, *320*, 365–376.
[4] J. P. Crow, J. S. Beckman, J. M. McCord, *Biochemistry* **1995**, *34*, 3544–3552.
[5] J. Winter, M. Ilbert, P. C. F. Graf, D. Özcelik, U. Jakob, *Cell* **2008**, *135*, 691–701.
[6] M. J. Gray, W.-Y. Wholey, B. W. Parker, M. Kim, U. Jakob, *J. Biol. Chem.* **2013**, *288*, 13789–13798.
[7] A. Perkins, D. A. Tudorica, M. R. Amieva, S. J. Remington, K. Guillemin, *PLOS Biol.* **2019**, *17*, e3000395.
[8] E. Bourlès, M. Isaac, C. Lebrun, J.-M. Latour, O. Sénèque, *Chem. – Eur. J.* **2011**, *17*, 13762–13772.
[9] V. Chabert, V. Lebrun, C. Lebrun, J.-M. Latour, O. Sénèque, *Chem. Sci.* **2019**, *10*, 3608–3615.
[10] R. Kassim, C. Ramseyer, M. Enescu, *Inorg. Chem.* **2011**, *50*, 5407–5416.
[11] M. Enescu, R. Kassim, C. Ramseyer, B. Cardey, *JBIC J. Biol. Inorg. Chem.* **2015**, *20*, 555–562.
[12] V. Lebrun, J.-L. Ravanat, J.-M. Latour, O. Sénèque, *Chem. Sci.* **2016**, *7*, 5508–5516.
[13] T. Dudev, C. Lim, *J. Am. Chem. Soc.* **2002**, *124*, 6759–6766.
[14] D. Picot, G. Ohanessian, G. Frison, *Comptes Rendus Chim.* **2009**, *12*, 546–553.
[15] J. Draper, K. Karplus, K. M. Ottemann, *J. Bacteriol.* **2011**, *193*, 4338–4345.
[16] M. Frisch et. al. *Gaussian 16 Revis. B01 Gaussian Inc Wallingford CT* **2016**. See S.I. for the full citation.
[17] A. D. Becke, *J. Chem. Phys.* **1993**, *98*, 5648–5652.
[18] M. Dolg, U. Wedig, H. Stoll, H. Preuss, *J. Chem. Phys.* **1987**, *86*, 866–872.
[19] V. A. Rassolov, J. A. Pople, M. A. Ratner, T. L. Windus, *J. Chem. Phys.* **1998**, *109*, 1223–1229.
[20] P. C. Hariharan, J. A. Pople, *Theor. Chim. Acta* **1973**, *28*, 213–222.
[21] R. Ditchfield, W. J. Hehre, J. A. Pople, *J. Chem. Phys.* **1971**, *54*, 724–728.
[22] Y. Zhao, D. G. Truhlar, *Theor. Chem. Acc.* **2008**, *120*, 215–241.
[23] Incorporating implicit solvation systematically increases barriers across all reaction coordinates and consequently leads to the same outcome and conclusions reported in the manuscript. See S.I. for more details.
[24] K. Fukui, *Acc. Chem. Res.* **1981**, *14*, 363–368.
[25] H. P. Hratchian, M. J. Frisch, *J. Chem. Phys.* **2011**, *134*, 204103.
[26] See S.I. for more details.
[27] X. Sheng, M. Kazemi, F. Planas, F. Himo, *ACS Catal.* **2020**, *10*, 6430–6449.
[28] With the chloride ion present, attempts at locating the zinc-bound sulfenic acid ligated at the S atom were unsuccessful and ultimately led to exchange of the sulfenic acid to form chloride-bound complexes (i.e., toward structure **6**). See S.I. for more details on IRC analysis.
[29] Similar ligand exchange to form zinc-bound halides have been experimentally observed as products of nucleophilic substitutions with synthetic zinc-bound thiolates. See: S.-J. Chiou, C. G. Riordan, A. L. Rheingold, *Proc. Natl. Acad. Sci.* **2003**, *100*, 3695–3700.
[30] C. Storkey, M. J. Davies, D. I. Pattison, *Free Radic. Biol. Med.* **2014**, *73*, 60–66.
[31] D. I. Pattison, M. J. Davies, *Chem. Res. Toxicol.* **2001**, *14*, 1453–1464.
[32] X. L. Armesto, M. Canle L, M. I. Fernández, M. V. García, J. A. Santaballa, *Tetrahedron* **2000**, *56*, 1103–1109.
[33] M. J. Davies, C. L. Hawkins, *Free Radic. Res.* **2000**, *33*, 719–729.
[34] P. Nagy, M. T. Ashby, *J. Am. Chem. Soc.* **2007**, *129*, 14082–14091.
[35] R. Taylor, O. Kennard, *J. Am. Chem. Soc.* **1982**, *104*, 5063–5070.
[36] G. R. Desiraju, *Acc. Chem. Res.* **1996**, *29*, 441–449.
[37] P. K. Thallapally, A. Nangia, *CrystEngComm* **2001**, *3*, 114–119.
[38] F. M. Bickelhaupt, K. N. Houk, *Angew. Chem. Int. Ed.* **2018**, 10070–10086.
[39] E. D. Glendening, C. R. Landis, F. Weinhold, *Wiley Interdiscip. Rev. Comput. Mol. Sci.* **2012**, *2*, 1–42.
[40] R. Kassim, C. Ramseyer, M. Enescu, *J. Biol. Inorg. Chem.* **2013**, *18*, 333–342.

Entry for the Table of Contents

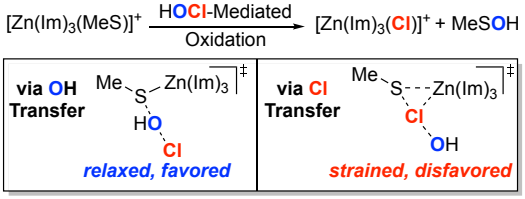

We report new reactivity and selectivity models for HOCl-mediated oxidation of zinc-bound thiolates predicated on minimizing geometric distortion at the zinc complex. We provide mechanistic insights into how gut-colonizing bacteria harness these complexes to sense and respond to host inflammation.